NATIONAL ADVISORY COMMITTEE FOR AERONAUTICS

WARTIME REPORT

ORIGINALLY ISSUED

June 1945 as
Advance Restricted Report No. 5C21

THEORETICAL INVESTIGATION OF METHODS FOR COMPUTING DRAG FROM WAKE SURVEYS AT HIGH SUBSONIC SPEEDS

By Max A. Heaslet

Ames Aeronautical Laboratory
Moffett Field, Calif.

NACA

WASHINGTON

NATIONAL ADVISORY COMMITTEE FOR AERONAUTICS

ADVANCE RESTRICTED REPORT

THEORETICAL INVESTIGATION OF METHODS FOR COMPUTING DRAG FROM WAKE SURVEYS AT HIGH SUBSONIC SPEEDS

By Max A. Heaslet

SUMMARY

In this report, graphs of constants are given which are to be used together with a knowledge of maximum total-head loss, static-pressure decrement, and the integral of total-head loss across the wake of an airfoil for the rapid determination of section profile-drag coefficient. The constants were computed under the assumption that the total-head pressure loss in the wake of the airfoil has a cosine-squared distribution and that no variation in static pressure exists across the wake at any given position. The range of pressure losses, for which the results are given, is sufficiently large for usual wind-tunnel and free-flight data, and compressibility effects are considered for Mach numbers up to and including $M = 1$, where M is the Mach number of the free stream.

Included in the report are results of computations that were carried out, for free-stream Mach numbers between 0.5 and 1.0 and for certain assumed types of total-pressure distribution in the wake, to compare theoretical drag coefficients as determined by various equations based upon the momentum method. Among the assumed wake shapes are forms similar to those encountered at supercritical speeds. Results obtained by point-by-point methods of integration are compared with those computed by means of the constants mentioned above. For the cases examined, the numerical agreement becomes less satisfactory as the maximum total-head decrement increases but for such total-head losses as are usually encountered in practice the agreement is quite sufficient. It is therefore concluded that, within the limits of the validity of the basic assumptions underlying the momentum method and for total-head decrements of normal magnitude, the use of the more rapid technique is justified

for wide variations in wake shapes for the Mach number range considered.

INTRODUCTION

One accepted method of determining the profile drag of an airfoil is developed from consideration of the momentum defect in the wake of the body. As given by Jones (reference 1), for velocities at which air may be assumed an incompressible medium, the actual computation involves the evaluation of an integral with integrand a function of total-head and static-pressure losses across the wake. In order to achieve this evaluation in terms of measured quantities, it is customary to presuppose that there is no mixing in the wake in stream tubes between the plane of measurement and a second plane which is far enough downstream that the static pressure there may be assumed to have returned to its original free-stream value.

When greater velocities are involved, it has been found possible to modify the Jones equation for compressibility effects so that the desired section drag may once more be found in terms of the same pressure measurements. As a counterpart to the previous assumption concerning mixing, it is again supposed that streamlines may be drawn in the wake, between the two planes, so that total head is constant along each stream tube. An added condition is necessary, however, in order that density may be evaluated and, to this end, the total energy per unit mass of air is assumed constant in any section across the field of flow.

The acceptance of the momentum method as a valid way of finding the drag of an airfoil section is dependent more on the experimental evidence at hand than on the unassailability of its underlying principles. In reference 2, G. I. Taylor has shown theoretically that, for certain types of pressure distributions, the indicated drag may be as much as 10 percent in error depending on whether the wake downstream mixes or flows in a streamline manner. In references 3 and 4, however, the method appears to have been substantiated experimentally by measurements taken at different distances behind the airfoil and by comparisons with values measured on a balance. The conclusions presented in reference 4 indicate that the values of drag

coefficient obtained by means of the momentum method are reliable up to speeds near the velocity of sound and that the presence of shock waves of limited extent does not invalidate the result. These conclusions must not be considered as a complete negation of Taylor's results, since his investigation of the pressure distributions encountered in practice, as given in reference 1, showed that the error due to mixing was in the worst case much smaller than was theoretically possible.

The expressions for drag coefficients, for either the compressible or incompressible case, appear as integrals which are to be evaluated in the measurement plane. Actual values of head loss and static-pressure variation can be determined by means of a pitot-traverse method and, as a consequence, the given integrals can be evaluated by numerical integration. In order to avoid the lengthy computation involved, an alternate approach has been developed by Silverstein and Katzoff (reference 5) in which it is assumed that drag is proportional to the integral of the total-head loss across the wake. The integral of head loss is obtained from an averaging rake, an integrating manometer, or by an integration of measurements made by a traversing tube. The proportionality factor, in turn, is evaluated by assuming a definite type of wake shape and, in this report, is tabulated as a function of maximum total-head loss, static-pressure decrement, and Mach number of the free stream. The results given herein deviate somewhat from those given in reference 5 for reasons that will be discussed later.

In reference 6 a comparison was made between values of drag coefficient computed by means of point-by-point integration and those determined by the integrating method and proportionality constants of reference 5. It was found that the latter procedure gave results in excellent agreement with those obtained by the former, at least up to values of the Mach number of the free stream in the neighborhood of 0.6. A wide range of shapes was considered and, remarkably enough, the agreement remained uniformly good for the Mach numbers considered.

Since in high-speed wind tunnels it is necessary to evaluate drag at Mach numbers above those considered in reference 6, and since the recalculation of the proportionality constants resulted in a change in their previously determined values, the present paper has undertaken the comparison of theoretical drag coefficients obtained

$$D = \rho_2 V_2 (V_0 - V_2)$$

$$C_D = \frac{D}{cq} = \frac{\rho_2 V_2 (V_2 - V_0)}{c \left(\frac{1}{2} \rho_0 V_0^2\right)}$$

$$= \frac{2}{c} \frac{\rho_2}{\rho_0} \frac{V_2}{V_0} \left(\frac{V_2 - V_0}{V_0}\right)$$

by different methods for the high-speed range. The appearance of shock waves on an airfoil may be expected at some value of free-stream Mach number less than unity and, as a consequence, the distribution of total-head loss differs considerably from that usually encountered. Some of the wake shapes considered are therefore chosen to correspond approximately to this situation.

OUTLINE OF METHOD

Complete details concerning the development of formulas for the drag coefficient may be found in the references. It is considered sufficient for the present purposes merely to list the main results. The symbols used are defined in the appendix.

In figure 1, the airfoil section is indicated together with the three planes of especial importance to the theory. Plane 0 is far enough upstream that free-stream conditions may be assumed to exist uniformly across this section. Plane 3 is at a great enough distance downstream that the value of static pressure has returned to its original value, p_0. Plane 1 is the actual plane of measurement.

From momentum considerations the drag d, per unit length of the airfoil, is

$$d = \int_w \rho_2 V_2 (V_0 - V_2) dy_2 \qquad (1)$$

where the integration across the wake is in plane 2. A proof of this relation, valid for subsonic compressible flow with possible limited shock waves, is given in reference 4.

The profile-drag coefficient for the airfoil section is an immediate consequence of equation (1), so that

$$c_d = \frac{2}{c} \int_w \frac{\rho_2}{\rho_0} \frac{V_2}{V_0} \left(1 - \frac{V_2}{V_0}\right) dy_2 \qquad (2)$$

If the fluid is assumed to be incompressible and continuous, and if no mixing is supposed to take place in the stream tubes between planes 1 and 2, equation (2) can be written as (a form of equation 2 can be)

$$c_d = \frac{2}{c}\int_w \sqrt{1-\frac{p_1-p_o}{H_o-p_o}-\frac{H_o-H_1}{H_o-p_o}}\left[1-\sqrt{1-\frac{H_o-H_1}{H_o-p_o}}\right]dy_1 \qquad (3)$$

From this form of the equation, the drag coefficient is directly calculable once the distributions of static-pressure and total-head loss across the wake are known.

If it is assumed, as Silverstein and Katzoff did in reference 5, that the integral of total-head loss across the wake is proportional to the section-drag coefficient, a proportionality constant F_1 may be introduced so that

$$c_d = \frac{F_1}{c}\int_w \frac{H_o-H_1}{H_o-p_o}\,dy_1 = F_1\,\frac{w}{c}\left(\frac{H_o-H_1}{H_o-p_o}\right)_{av} \qquad (4)$$

where the subscript av. denotes average value across the wake. In references 5 and 6, F_1 is tabulated as computed from equations (3) and (4) under the supposition that $\frac{p_1-p_o}{H_o-p_o}$ is constant and that $\frac{H_o-H_1}{H_o-p_o}$ has a cosine-squared distribution; that is,

$$\frac{H_o-H_1}{H_o-p_o} = \left(\frac{H_o-H_1}{H_o-p_o}\right)_{max}\cos^2\frac{\pi y}{w}$$

where $|y| \leq \frac{w}{2}$ and is measured from the center line of the wake. In figures 2(a) and 2(b) extended values of F_1 are given in graphical form as functions of $\frac{p_1-p_o}{H_o-p_o}$ and $\left(\frac{H_o-H_1}{H_o-p_o}\right)_{max}$.

When compressibility effects are to be considered, factors F_c or F_c/F_i are used, so that

$$c_d = \frac{F_c}{c}\int_w \frac{H_o - H_i}{H_o - p_o}\,dy_i = \frac{F_c}{F_i}\left[F_i\,\frac{w}{c}\left(\frac{H_o - H_i}{H_o - p_o}\right)_{av}\right] \quad (5)$$

The evaluation of F_c is similar to that of F_i and proceeds as follows: Equation (2) is rewritten in such a form that the integrand may be calculated directly from the free-stream Mach number, the static-pressure loss, and the total-head loss in the wake. If constant values of the first two parameters and a cosine-squared distribution of the latter are assumed, it is possible to find c_d and subsequently to solve equation (3) for F_c. In figures 3(a) to 3(e) will be found F_c/F_i plotted as a function of M, $\left(\frac{H_o - H_i}{H_o - p_o}\right)_{max}$, and $\frac{p_i - p_o}{H_o - p_o}$.

In this report, two forms of equation (2) are used in the point-by-point integration for the compressible case. The first expression,

$$c_d = \frac{2}{c}\int_w \left(\frac{H_i}{H_o}\right)^{\frac{\gamma-1}{\gamma}} \left(\frac{p_i}{p_o}\right)^{\frac{1}{\gamma}} \left\{\frac{1-\left(\frac{p_i}{H_i}\right)^{\frac{\gamma-1}{\gamma}}}{1-\left(\frac{p_o}{H_o}\right)^{\frac{\gamma-1}{\gamma}}}\right\}^{\frac{1}{2}} \left\{1-\left[\frac{1-\left(\frac{p_o}{H_i}\right)^{\frac{\gamma-1}{\gamma}}}{1-\left(\frac{p_o}{H_o}\right)^{\frac{\gamma-1}{\gamma}}}\right]^{\frac{1}{2}}\right\} dy_i \quad (6)$$

is derived in reference 4 under the assumptions that total energy per unit mass of air is constant in any section across the field of flow and that between planes (1) and (2) Bernoulli's equation for compressible flow holds. This form has a great advantage in that auxiliary tables, which are included in the reference, may be prepared so that the computations involved are expedited.

As derived in reference 6, the alternate form of the expression for drag coefficient is

$$c_d = \frac{2}{c}\int_w \sqrt{\left(\frac{p_i}{p_o}\right)^{\frac{1}{\gamma}}\left(\frac{H_1-p_1}{H_o-p_o}\right)\left(\frac{1+\eta_2}{1+\eta_1}\right)}\left[\sqrt{\frac{1+\frac{\gamma-1}{2}M^2\left(\frac{H_1-p_o}{H_o-p_o}\right)\left(\frac{1+\eta_o}{1+\eta_1}\right)}{1+\frac{\gamma-1}{2}M^2}} - \sqrt{\left(\frac{H_1-p_o}{H_o-p_o}\right)\left(\frac{1+\eta_o}{1+\eta_2}\right)}\right] dy_1 \quad (7)$$

The expression $1+\eta$, which appears in equation (7), is the so-called compressibility factor and is a function of Mach number,

$$1+\eta = 1 + \frac{M^2}{4} + \frac{M^4}{40} + \frac{M^6}{1600} - \frac{M^8}{80000} + \ldots$$

Figure 4 shows this function, for values of M up to 1, in a form that can be used in numerical integration. The subscripts on η, as given in equation (7), indicate the plane in which M is evaluated.

One outstanding simplification possible in the integration of equation (7) was made by Ray H. Wright of the Langley Memorial Aeronautical Laboratory in some unpublished results. If the second radical, in the integrand of this equation, is written in the form

$$1 - G\left(1 - \frac{q_2}{q_o}\right)$$

it may be shown that G is primarily a function of Mach number and secondarily dependent on $1 - \frac{q_2}{q_o}$. This follows from the definition of G, for

$$G = \frac{1 - \sqrt{\dfrac{1 + \dfrac{\gamma - 1}{2} M^2 \dfrac{q_a}{q_0}}{1 + \dfrac{\gamma - 1}{2} M^2}}}{1 - \dfrac{q_a}{q_0}} = \frac{1}{2}\left(\frac{\dfrac{\gamma-1}{2} M^2}{1 + \dfrac{\gamma-1}{2} M^2}\right)$$

$$+ \left(\frac{\dfrac{\gamma-1}{2} M^2}{1+\dfrac{\gamma-1}{2} M^2}\right)^2 \frac{\left(1 - \dfrac{q_a}{q_0}\right)}{8} + \left(\frac{\dfrac{\gamma-1}{2} M^2}{1+\dfrac{\gamma-1}{2} M^2}\right)^3 \frac{\left(1 - \dfrac{q_a}{q_0}\right)^2}{16} + \cdots$$

A graphical representation of G is given in figure 5.

When proceeding to the actual integration, it is sufficient to know the variation of $\frac{H_0 - H_1}{H_0 - p_0}$, the Mach number of the free stream, and the value of $\frac{p_1 - p_0}{H_0 - p_0}$. In the computation it will be found necessary to use the indicated pressure ratio $\frac{H_0 - p_0}{p_0}$. Figure 6 gives values of this parameter as a function of free-stream Mach number, M.

As mentioned previously, the values of F_0/F_1 in figures 3(a) to 3(e) differ in most cases from the corresponding values given in reference 5. Since the original assumptions are the same, there seems little doubt that this discrepancy is produced by differences in the manner in which the integration of the basic equation is performed. This report assumes a distribution for total-head decrement $\frac{H_0 - H_1}{H_0 - p_0}$; while reference 5 assumes a distribution for velocity-squared decrement $\frac{V_0^2 - V_2^2}{V_0^2}$, although the precise nature of this latter assumption is not stated explicitly. An analysis of the two sets of results gives

credence to the conclusion that Silverstein and Katzoff have set

$$\frac{H_0 - H_1}{H_0 - p_0} = \frac{V_0^2 - V_2^2}{V_0^2}$$

which is in agreement with the theory of incompressible fluids. Such a relationship does not introduce large errors unless the Mach number is of considerable magnitude, but in this latter case the relation is untenable and the values of F_c/F_i in this report would appear to be the true values. These remarks apply equally well to reference 6, since the graphs of F_c/F_i given there are in agreement with the tabular data in reference 5.

COMPUTATIONS

By means of the graphical data that have been presented, and the tables included in reference 4, it is now possible to determine values of drag coefficient from equations (5), (6), and (7) and known wake distributions. Such data can, in turn, be used for a comparison of the results obtained from point-by-point methods of integration and the Silverstein and Katzoff integrating method.

In the five cases listed below, an arbitrary distribution for $\frac{H_0 - H_1}{H_0 - p_0}$ is assumed, together with fixed values for $\frac{p_1 - p_0}{H_0 - p_0}$. The drag coefficient is then computed for different values of free-stream Mach number. In choosing the wake forms, all of which are shown in figures 7(a) and 7(b), an attempt was made in cases I, III, and IV to present distributions that are highly distorted from usual distributions; while in cases II and V shapes were chosen that resembled somewhat the types encountered when shock waves are present on the surface of the airfoil.

It will be noted that all the cases are concerned with symmetrical configurations. Typical asymmetrical shapes could be constructed by joining two halves of cosine-squared distributions with equal heights and different base

widths. From the theory underlying the derivation of constants F_i and F_c/F_i, it follows that for such typical asymmetrical shapes the values of drag coefficient given by equations (4) and (5) will always be exact. Other forms of asymmetry may be thought of as deviations from these hybrid cosine-squared curves and the study of the variation in drag coefficient produced by these deviations can be related directly to problems such as are considered here.

Case I

As an extreme example, the distribution of head loss is made rectangular. Thus, as shown in figure 7(a), let $\frac{H_o - H_1}{H_o - p_o} = 0.10$ for $|y| \leq c$ and equal to zero for all other values of y; moreover, let $\frac{p_1 - p_o}{H_o - p_o} = 0.1$. It follows immediately that

$$\frac{1}{c}\int_w \frac{H_o - H_1}{H_o - p_o}\,dy = 0.20$$

In table I, results of the computations are given.

Equations (6) and (7) should give the same numerical result since they are equivalent. The deviations that appear are probably attributable for the most part to small errors arising in reading the graphs and, to a smaller extent, to the interpolation necessary in the tables. The differences in results from equations (5) and (6) are probably due to the variation between the actual wake form and the hypothetical shape used to compute F_c/F_i although numerical inaccuracies must again be considered. It is observed, however, that the percentage of error is small.

Case II

The distribution of head loss for this case is shown in figure 7(a). Under the assumption that $\frac{p_1 - p_o}{H_o - p_o} = 0.1$, the drag coefficient has been computed by means of equations (5) and (7) for different Mach numbers. The results of these calculations are given in table II

and show that in each instance the error in the data determined by equation (5) is small.

Case III

Assume now that $\frac{H_o - H_1}{H_o - p_o} = 0.30$ for $|y| \leq \frac{1}{8} c$, as shown in figure 7(a). In table III, drag coefficients are given corresponding to this distribution of head loss when $\frac{p_1 - p_o}{H_o - p_o} = 0.1, 0.0, -0.2, -0.4$, respectively, and for various Mach numbers. The calculations are based on equations (5) and (6). The disparities between corresponding answers are, in general, larger for these examples than in case I. On the other hand, the percentage of error seems relatively small in comparison with the deviation between the true and assumed wake shape.

Case IV

In this case, drag coefficient is computed from equations (5) and (6) when $M = 0.4, 0.6, 0.8$, and 1.0 under the assumption that $\frac{H_o - H_1}{H_o - p_o} = 0.10$ for $|y| \leq \frac{c}{8}$ as shown in figure 7(b). Table IV lists the results for $\frac{p_1 - p_o}{H_o - p_o} = 0.0, -0.1, -0.2$, and -0.4, and in each case the percentage of error is small.

Case V

For the distribution of $\frac{H_o - H_1}{H_o - p_o}$ shown in figure 7(b) and for $\frac{p_1 - p_o}{H_o - p_o} = 0, -0.2$, and -0.4, drag coefficient is computed at free stream Mach numbers equal to 0.4, 0.6, 0.8, and 1.0. In this case the maximum total-head loss is 0.7 and, as can be seen in table V, the percentage of error is quite large, especially for higher values of $\frac{p_1 - p_o}{H_o - p_o}$.

CONCLUSIONS

The computations carried out in this report show that the integrating method of Silverstein and Katzoff gives results in good agreement with the values of drag coefficient computed by the much more laborious process of point-by-point integration so long as the maximum total-head loss is not too large. The limitation on the total-head loss is necessarily dependent on the accuracy desired, but for such values as are usually encountered in practice the cases considered do not show exorbitant deviations in the results.

The agreement in results holds for considerable variation of the wake form and, as far as theoretical results are concerned, extends up to a free-stream Mach number equal to 1. Since previous reports have indicated that the momentum method is not necessarily nullified by the existence of shock waves of limited extent, it follows that the integrating method need not be invalid beyond the critical speed of the airfoil.

Ames Aeronautical Laboratory,
National Advisory Committee for Aeronautics,
Moffett Field, Calif.

APPENDIX

SYMBOLS

V	velocity
p	static pressure
q	dynamic pressure
H	total pressure
ρ	density
c	chord length of airfoil
y	distance measured vertically from wake center
w	wake width
M	Mach number, ratio of the stream velocity to the local velocity of sound
d	section profile drag
c_d	section profile-drag coefficient
F_c	proportionality constant for compressible flow
F_i	proportionality constant for incompressible flow
$1+\eta$	compressibility correction factor, $q = \rho \frac{V^2}{2} = \frac{H-p}{1+\eta}$
γ	ratio of specific heat at constant pressure to specific heat at constant volume

Subscripts 0, 1, 2, refer to conditions existing in three different planes. Subscript 0 denotes free-stream conditions, 1 denotes the plane of measurement, and 2 denotes the plane aft of the airfoil in which the static pressure has returned to its free-stream value.

REFERENCES

1. The Cambridge University Aeronautics Laboratory: The Measurement of Profile Drag by the Pitot-Traverse Method. R. & M. No. 1688, British A.R.C., 1936.

2. Taylor, G. I.: The Determination of Drag by the Pitot Traverse Method. R. & M. No. 1808, British A.R.C., 1937.

3. Goett, Harry J.: Experimental Investigation of the Momentum Method for Determining Profile Drag. NACA Rep. No. 660, 1939.

4. Lock, C. N. H., Hilton, W. F., and Goldstein, S.: Determination of Profile Drag at High Speeds by a Pitot Traverse Method. British A.R.C. 4709 (Ae. 1708), (British Confidential - U.S. Restricted), Sept. 19, 1940.

5. Silverstein, A., and Katzoff, S.: A Simplified Method for Determining Wing Profile Drag in Flight. Jour. Aero. Sci., vol. 7, no. 7, May 1940, pp. 295-301.

6. Davis, Wallace F.: Comparison of Various Methods for Computing Drag from Wake Surveys. NACA ARR, Jan. 1943.

TABLE I.- c_d AS A FUNCTION OF MACH NUMBER

FOR WAKE FORM IN CASE I

Mach number	c_d (equation (7))	c_d (equation (6))	c_d (equation (5))	Percentate of error in equation (5) as compared with equation (6)
0.5	0.1678	0.1678	0.1687	0.5
.6	.1614	.1616	.1624	.5
.7	.1550	.1551	.1556	.3
.8	.1474	.1476	.1483	.5
.9	.1400	.1403	.1409	.4
1.0	.1334	.1331	.1333	.2

TABLE II.- c_d AS A FUNCTION OF MACH NUMBER

FOR WAKE FORM IN CASE II

Mach number	c_d (equation (7))	c_d (equation (5))	Percentage of error in equation (5) as compared with equation (7)
0.6	0.1589	0.1589	0
.7	.1532	.1528	-.3
.8	.1461	.1455	-.4
.9	.1391	.1385	-.4
1.0	.1324	.1313	-.8

TABLE III.- c_d AS A FUNCTION OF MACH NUMBER FOR WAKE FORM IN CASE III

$\frac{p_1-p_o}{H_o-p_o}$	Mach number	c_d Equation (6)	c_d Equation (5)	Percentage of error in equation (5) as compared with equation (6)
0.1	0.4	0.0603	0.0621	3.0
.1	.6	.0570	.0584	2.5
.1	.8	.0529	.0540	2.1
.1	1.0	.0485	.0490	1.0
0	.4	.0648	.0662	2.2
0	.6	.0607	.0617	1.6
0	.8	.0556	.0562	1.1
0	1.0	.0500	.0501	0.2
-.2	.4	.0725	.0734	1.2
-.2	.6	.0667	.0672	-.7
-.2	.8	.0593	.0593	0
-.2	1.0	.0508	.0505	-.6
-.4	.4	.0792	.0795	.4
-.4	.6	.0714	.0714	0
-.4	.8	.0612	.0608	-.7
-.4	1.0	.0471	.0464	-1.5

TABLE IV.- c_d AS A FUNCTION OF MACH NUMBER FOR WAKE FORM IN CASE IV

$\frac{p_1-p_o}{H_o-p_o}$	Mach number	c_d Equation (6)	c_d Equation (5)	Percentage of error in equation (5) as compared with equation (6)
0	0.4	0.0228	0.0229	0.4
0	.6	.0211	.0212	.5
0	.8	.0190	.0190	0
0	1.0	.0168	.0168	0
-.1	.4	.0239	.0240	.4
-.1	.6	.0219	.0220	.5
-.1	.8	.0195	.0195	0
-.1	1.0	.0168	.0168	0
-.2	.4	.0249	.0250	.4
-.2	.6	.0226	.0226	0
-.2	.8	.0198	.0198	0
-.2	1.0	.0167	.0166	-.6
-.4	.4	.0267	.0268	.4
-.4	.6	.0238	.0238	0
-.4	.8	.0201	.0200	-.5
-.4	1.0	.0151	.0150	-.7

TABLE V.- c_d AS A FUNCTION OF MACH NUMBER FOR WAKE FORM IN CASE V

$\frac{p_1-p_o}{H_o-p_o}$	Mach number	c_d Equation (6)	c_d Equation (5)	Percentage of error in equation (5) as compared with equation (6)
0	0.4	0.1046	0.0967	-7.7
0	.6	.0982	.0919	-6.4
0	.8	.0902	.0860	-4.7
0	1.0	.0814	.0792	-2.7
-.2	0.4	0.1196	0.1149	-3.9
-.2	.6	.1102	.1076	-2.4
-.2	.8	.0983	.0976	-.7
-.2	1.0	.0846	.0858	1.4
-.4	0.4	0.1318	0.1299	-1.4
-.4	.6	.1192	.1194	.2
-.4	.8	.1027	.1043	1.6
-.4	1.0	.0799	.0829	3.8

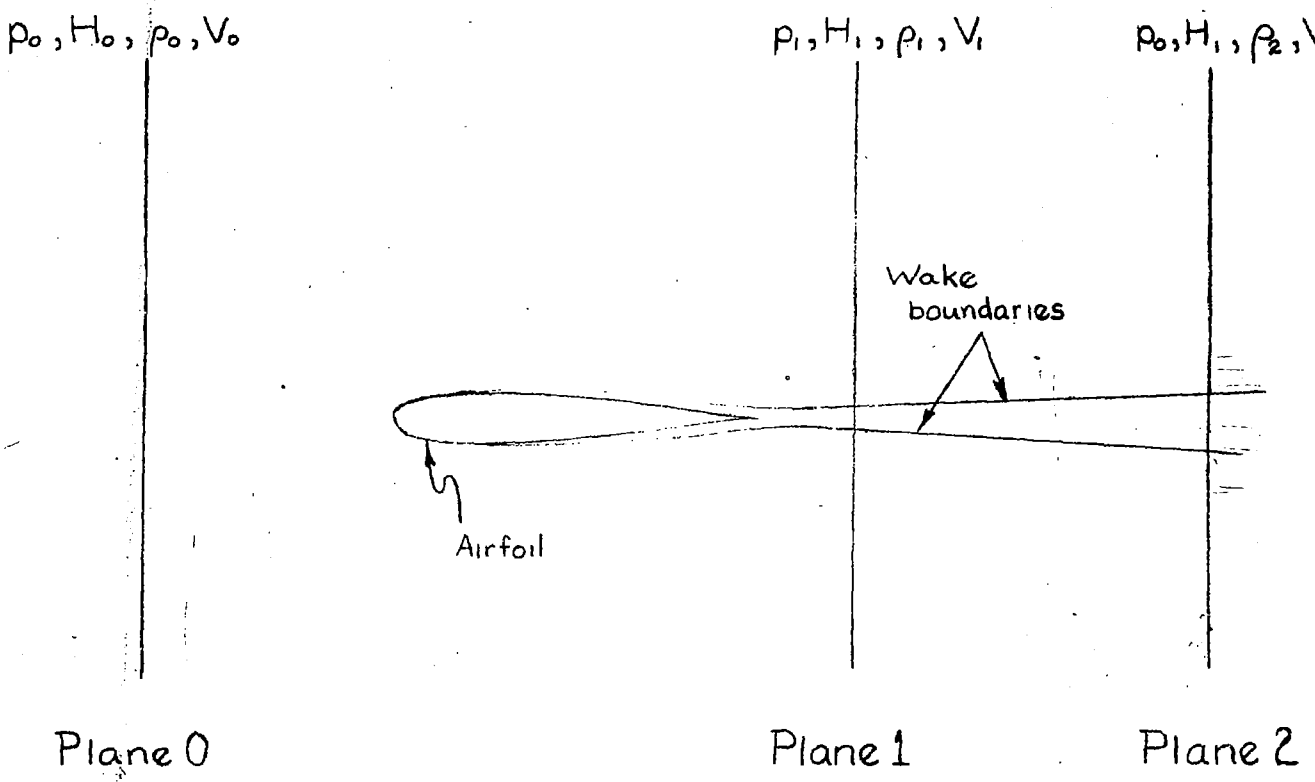

NATIONAL ADVISORY COMMITTEE
FOR AERONAUTICS

FIGURE 1 - DIAGRAM OF AIRFOIL, WITH WAKE, IN A COMPRESSIBLE FLUID

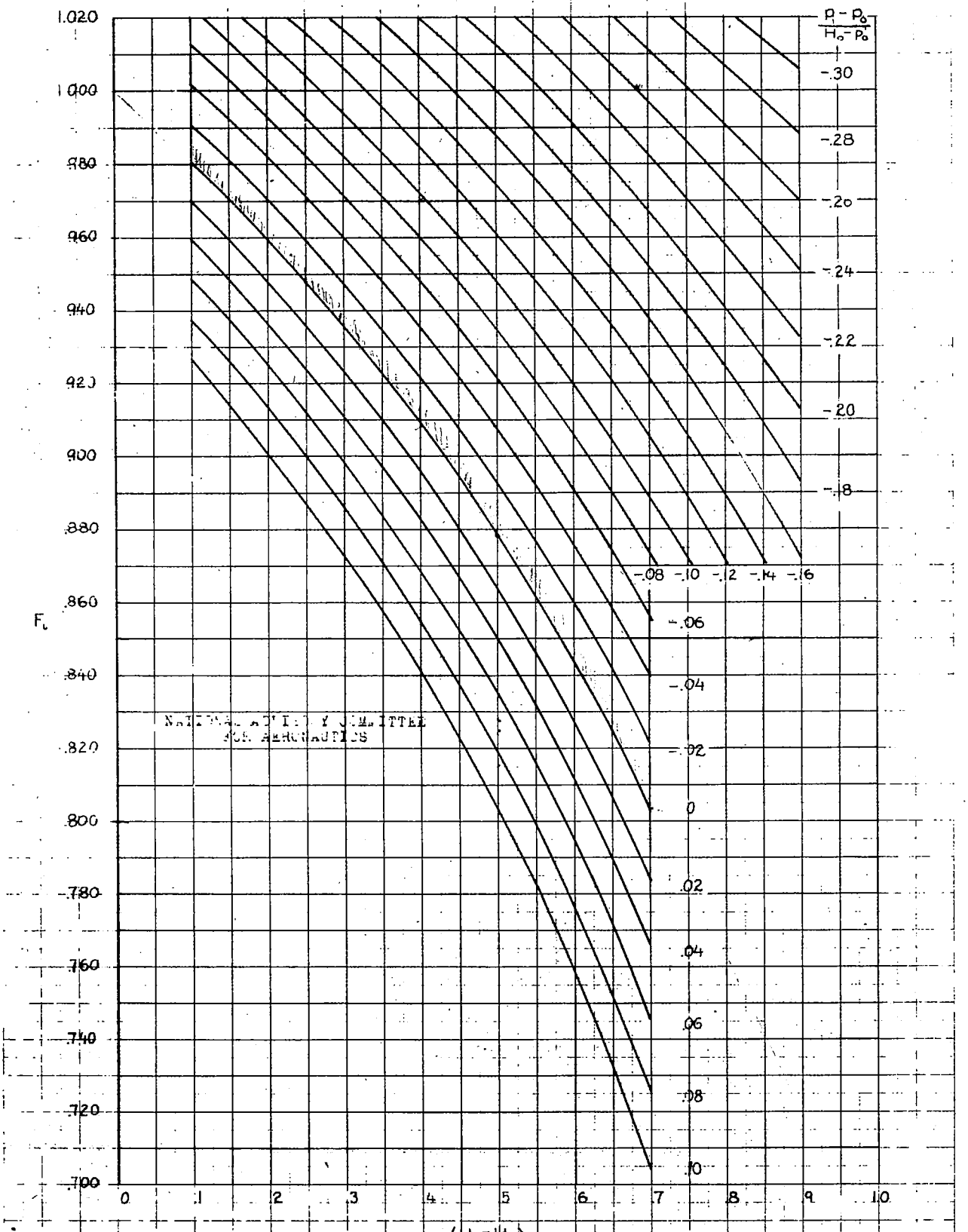

FIGURE 2. - F_t AS A FUNCTION OF $\left(\frac{H_o - H_1}{H_o - p_o}\right)_{max.}$ AND $\left(\frac{p_1 - p_o}{H_o - p_o}\right)$ (a) $\left(\frac{p - p_o}{H_o - p_o}\right)$ RANGING FROM .10 TO -.30.

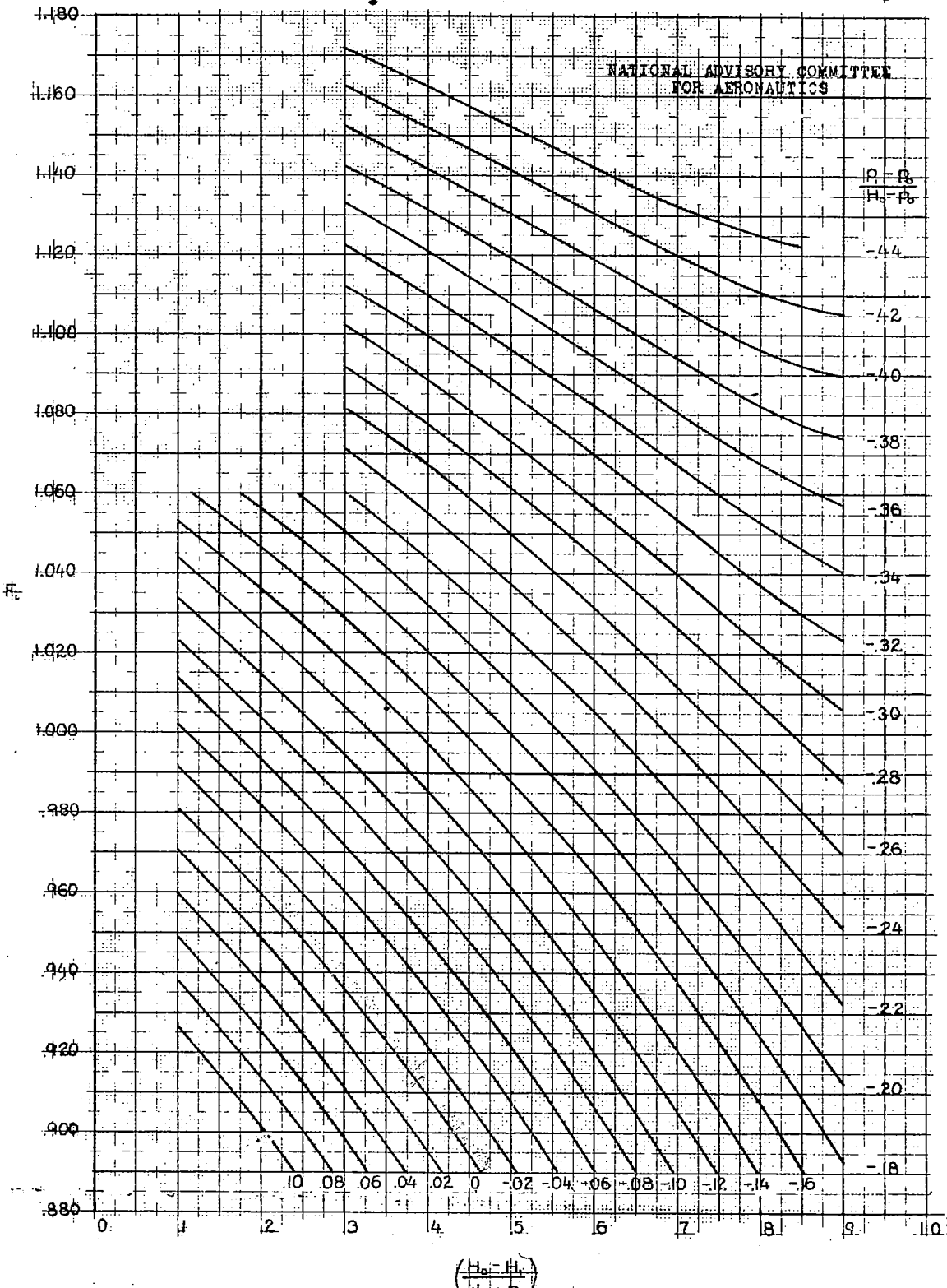

FIGURE 2 - E_t AS A FUNCTION OF $\left(\frac{H_0 - H_1}{H_0 - p_0}\right)_{max.}$ AND $\left(\frac{p_1 - p_0}{H_0 - p_0}\right)$ (b) $\left(\frac{p_1 - p_0}{H_0 - p_0}\right)$ RANGING FROM .10 TO -.44.

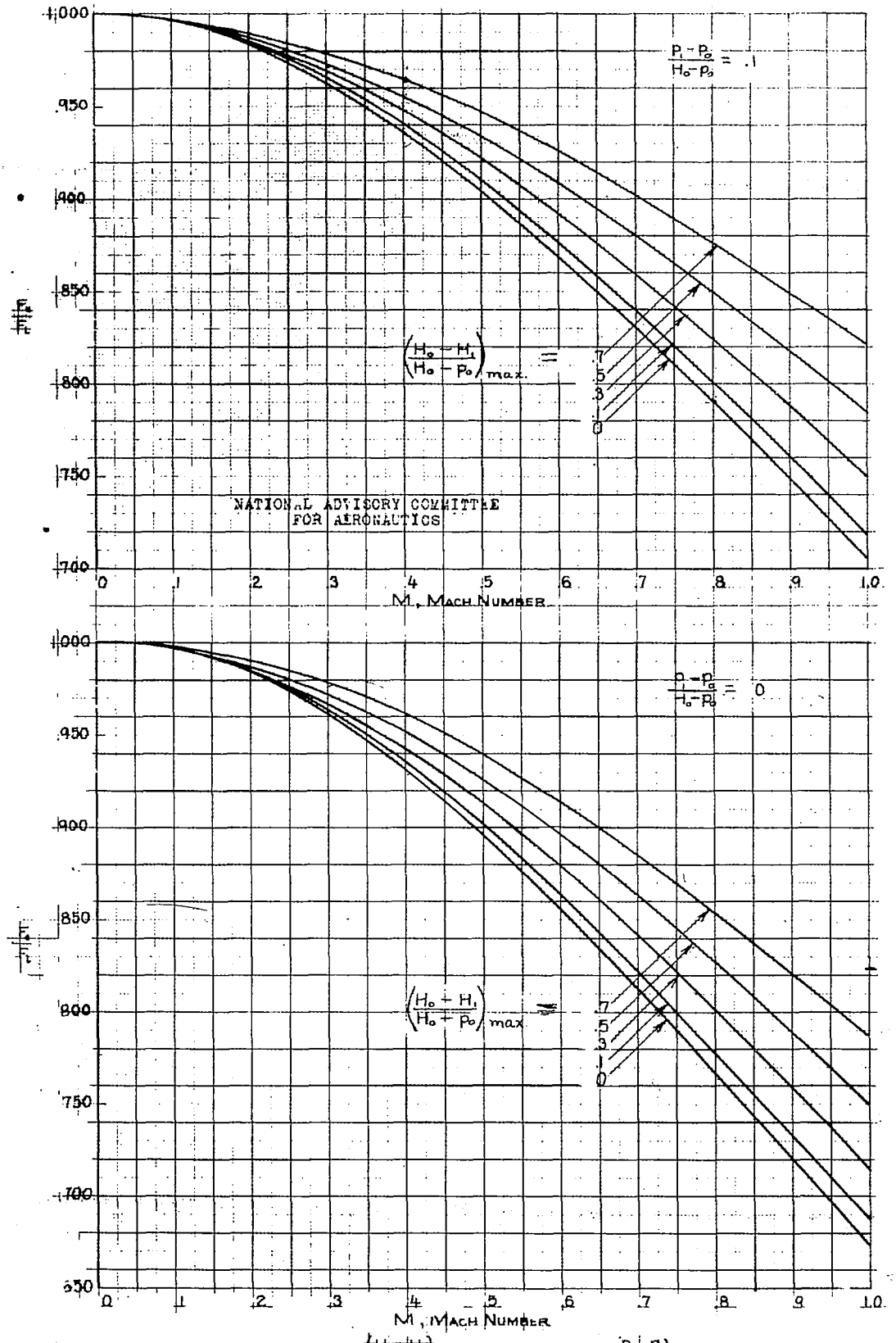

FIGURE 3.- $\frac{P_1}{P_0}$ AS A FUNCTION OF $\left(\frac{H_0 - H_1}{H_0 - P_0}\right)_{max.}$ AND M, (α), $\left(\frac{P_1 - P_0}{H_0 - P_0}\right)$ EQUAL TO .1 AND 0.

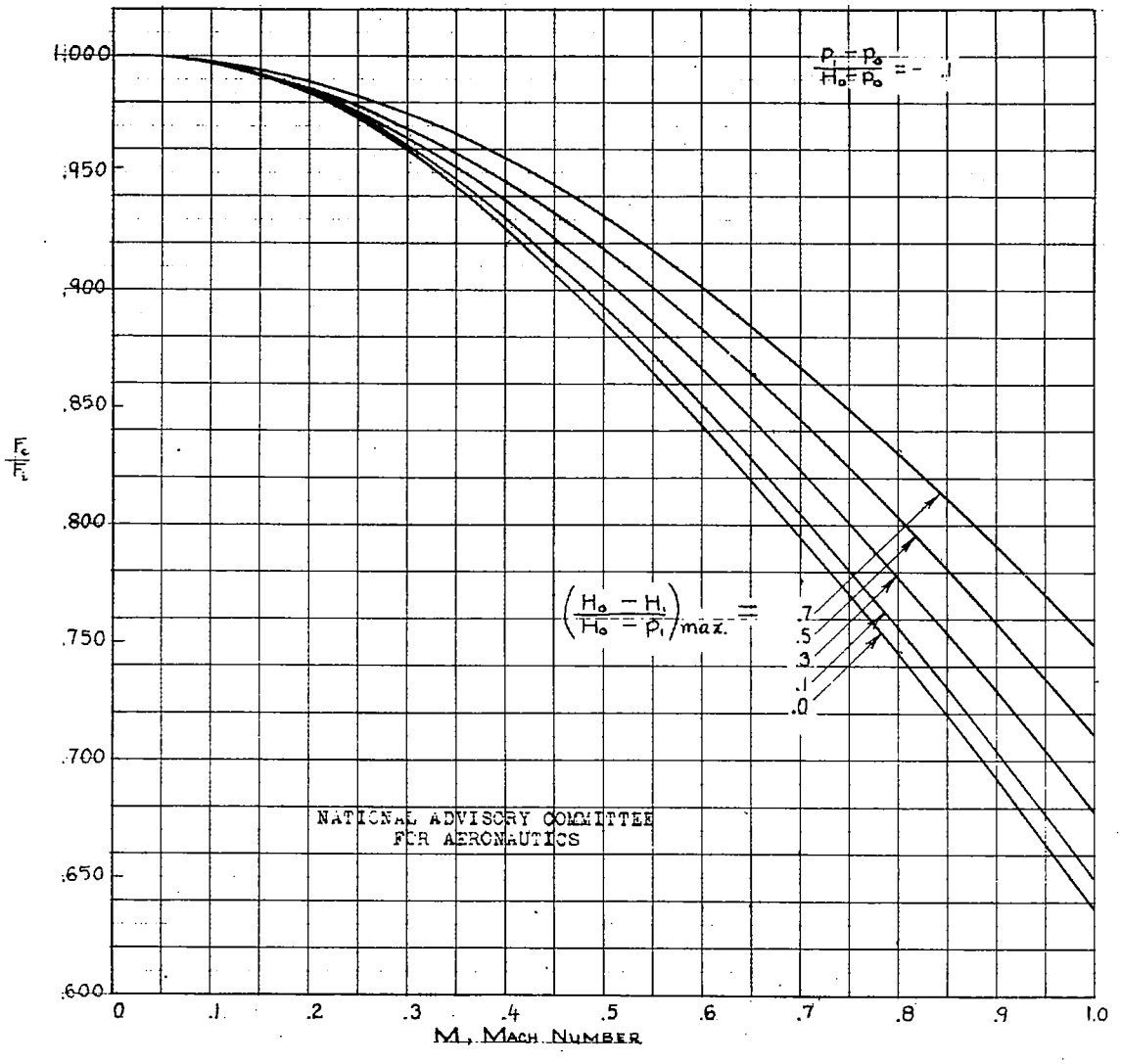

FIGURE 3.- F_o/F_i AS A FUNCTION OF $\left(\frac{H_o - H_i}{H_o - p_o}\right)_{max.}$, AND M. (b) $\left(\frac{p_i - p_o}{H_o - p_o}\right)$ EQUAL TO - .1.

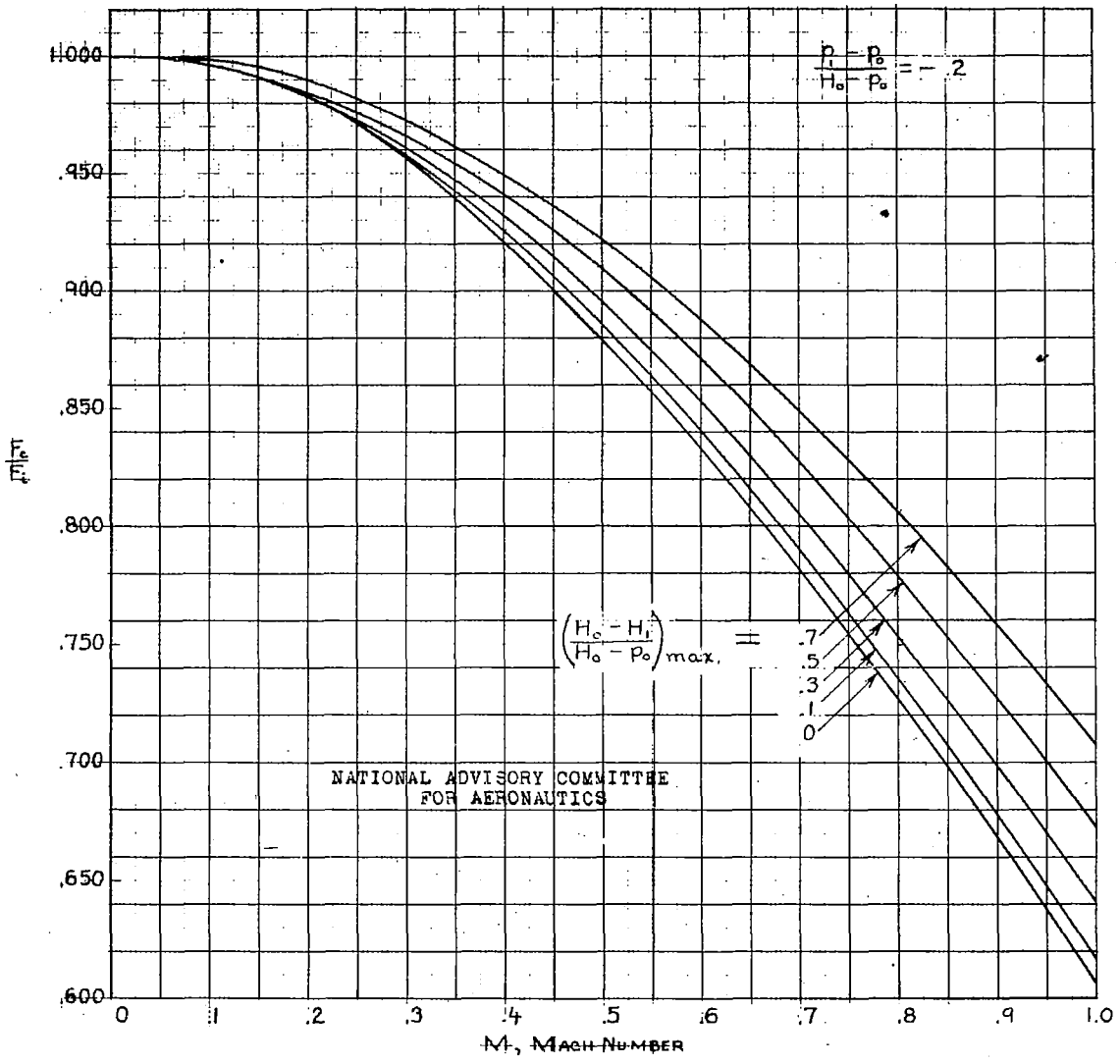

FIGURE 3.- F_c/F_i AS A FUNCTION OF $\left(\frac{H_0 - H_1}{H_0 - p_0}\right)_{max.}$, AND M. (c) $\left(\frac{p_1 - p_0}{H_0 - p_0}\right)$ EQUAL TO -.2.

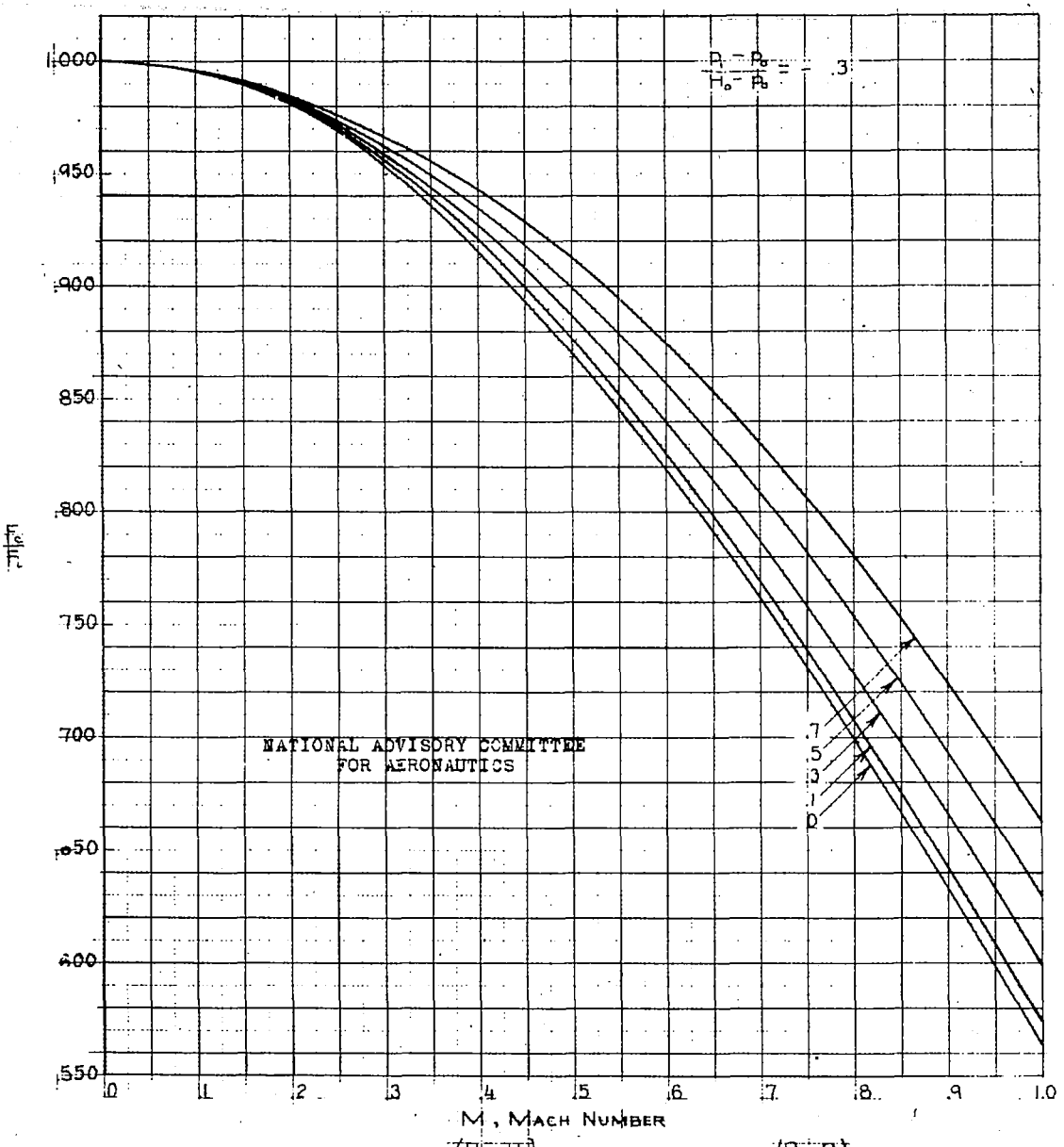

FIGURE 3.- $\frac{F_c}{F_t}$ AS A FUNCTION OF $\left(\frac{H_b - H_1}{H_b - P_a}\right)_{max}$, AND M. (d) $\left(\frac{P_1 - P_o}{H_o - P_o}\right)$ EQUAL TO - .3.

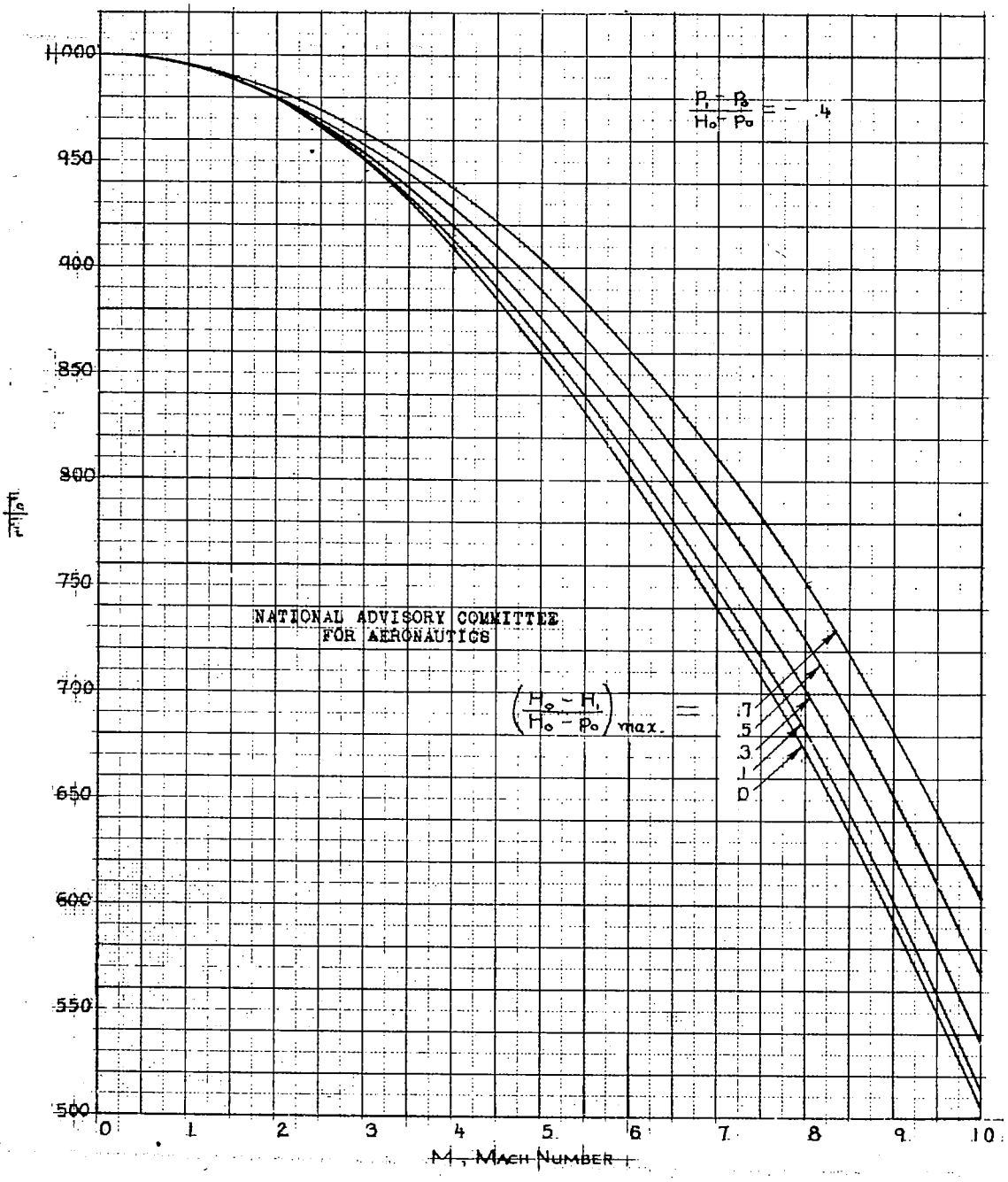

FIGURE 3.- $\frac{F_c}{F_i}$ AS A FUNCTION OF $\left(\frac{H_0 - H_1}{H_0 - P_0}\right)_{max.}$ AND M. (e) $\left(\frac{P_1 - P_0}{H_0 - P_0}\right)$ EQUAL TO -.4.

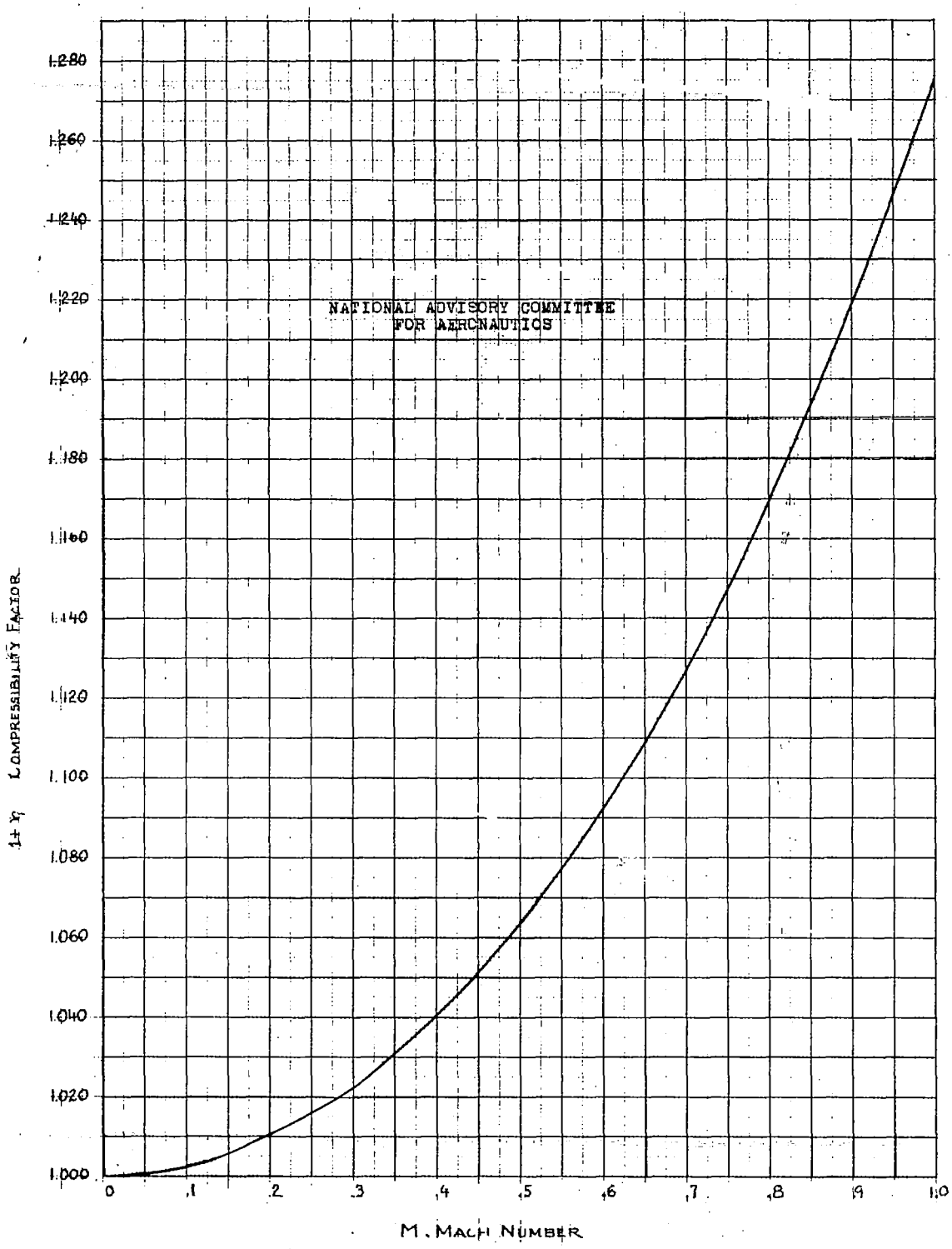

FIGURE 4.- COMPRESSIBILITY FACTOR, $1+\eta$, AS A FUNCTION OF MACH NUMBER, M.

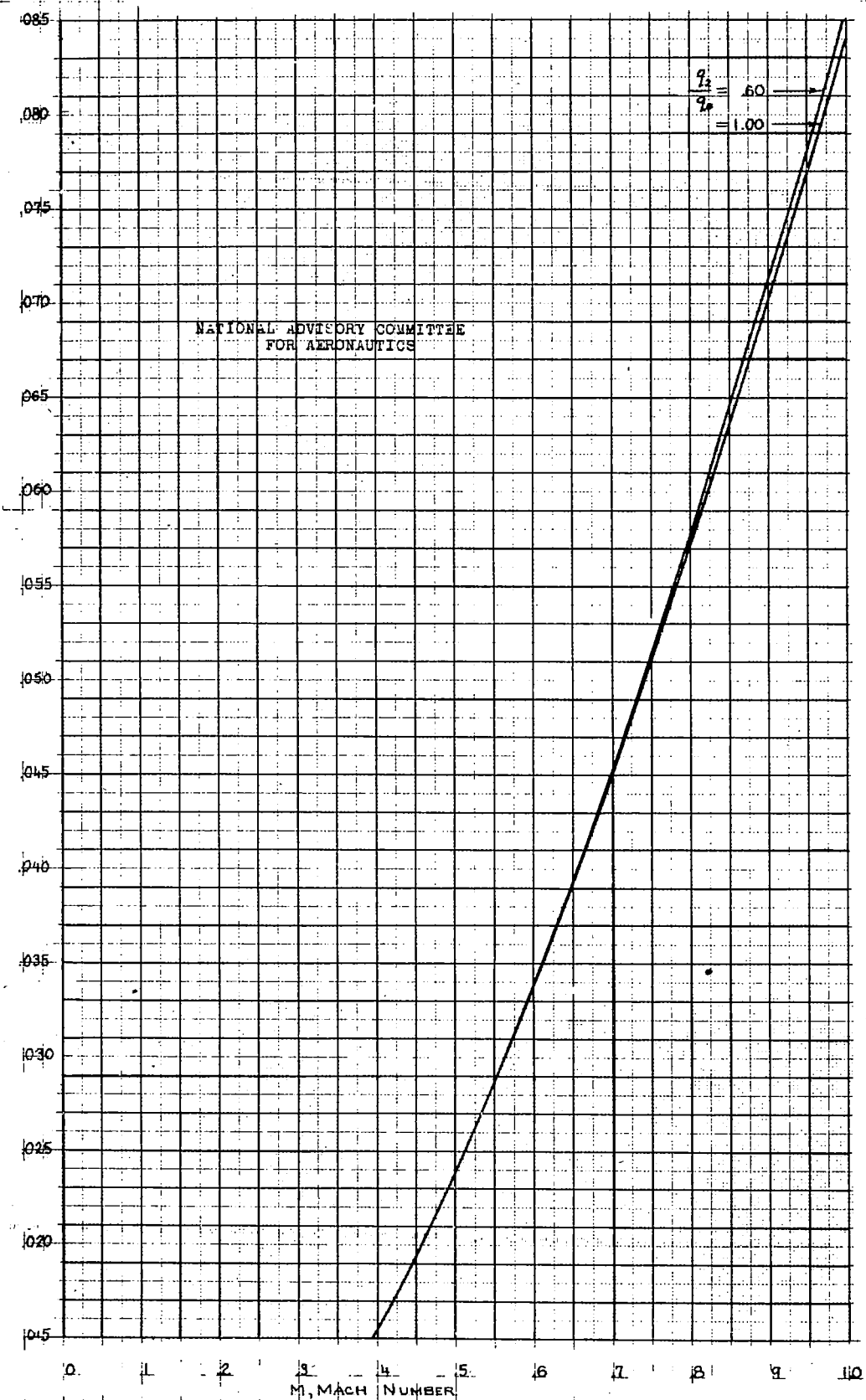

FIGURE 5.- G VERSUS MACH NUMBER, M, AND RATIO OF DYNAMIC PRESSURES, q_2/q_0.

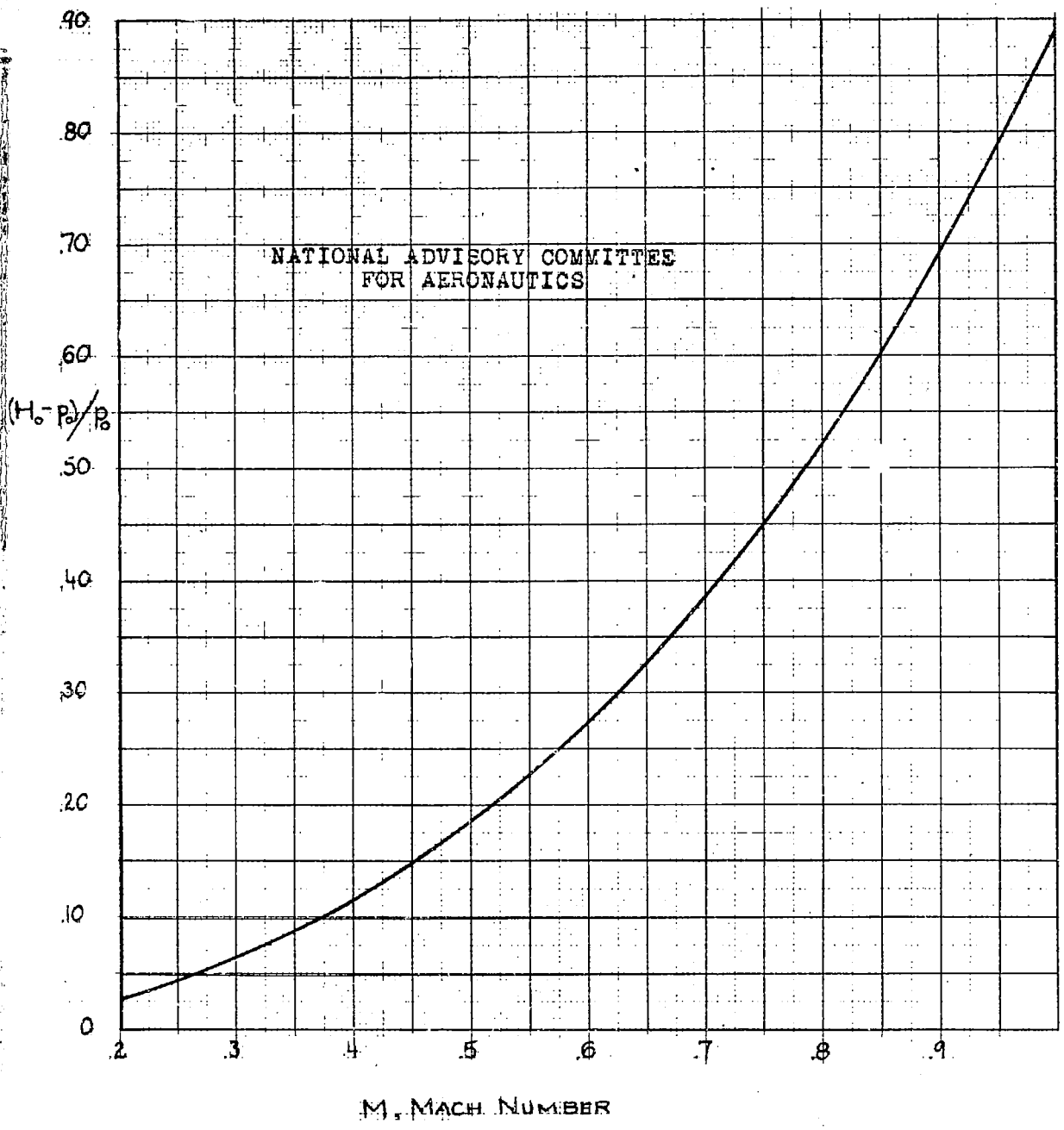

FIGURE 6 - INDICATED PRESSURE RATIO, $(H_0 - p_0)/p_0$, VERSUS MACH NUMBER, M.

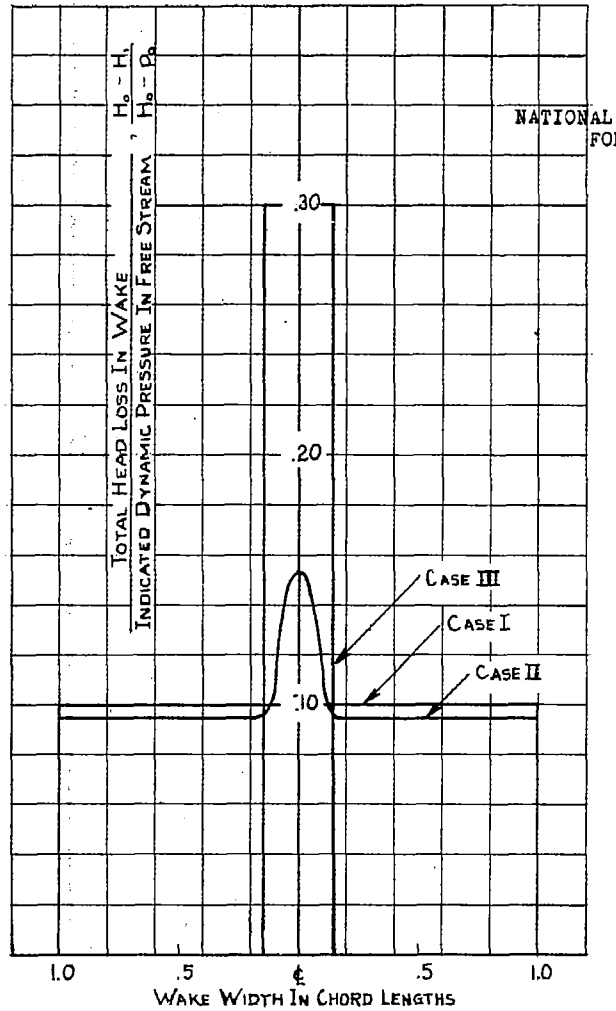

FIGURE 7. - TYPES OF WAKE SHAPES EMPLOYED.
(a) CASES I, II, AND III.

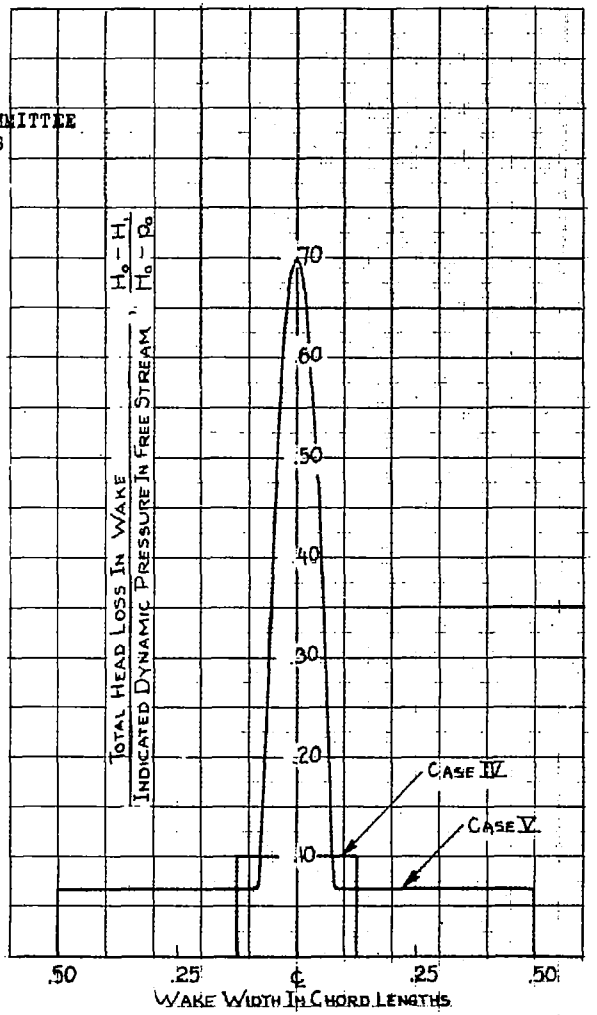

FIGURE 7. - TYPES OF WAKE SHAPES EMPLOYED.
(b) CASES IV AND V